Numerical Study of the Succession of Attractors in the Periodically Forced Rayleigh System

Petre Băzăvan

ABSTRACT. The autonomous second order nonlinear ordinary differential equation (ODE) $\ddot{x} + \frac{\dot{x}^3}{3} - \dot{x} + x = 0$, introduced in 1883 by Lord Rayleigh, is the nonlinear equation in $\dot{x}$ which appears to be the closest to the ODE of the harmonic oscillator with dumping [Diener, 1979, 1].

In this paper we present a numerical study of the periodic and chaotic attractors in the dynamical system associated with the generalized Rayleigh equation $\varepsilon \ddot{x} + \frac{\dot{x}^3}{3} - \dot{x} + ax = g \sin \omega t$. Numerical results describe the system dynamics changes (in particular bifurcations), when the forcing frequency is varied and thus, periodic or chaotic behavior regions are predicted.

2000 Mathematics Subject Classification. 34K28, 37C50, 37C70, 37G15, 37M20.
Key words and phrases. periodic and chaotic attractors, bifurcations, Poincaré map and sections, Lyapunov exponents, basin boundaries metamorphoses.

1. Introduction

The nonautonomous second order nonlinear ODE with time dependent sinusoidal forcing term, given by Diener [1979, 1],

$$\varepsilon \ddot{x} + \frac{\dot{x}^3}{3} - \dot{x} + ax = g \sin \omega t, \tag{1}$$

is a generalisation of the Rayleigh equation $\ddot{x} + \frac{\dot{x}^3}{3} - \dot{x} + x = 0$ [Diener, 1979, 1]. Here, $x : \mathbb{R} \to \mathbb{R}$, $x = x(t)$ is the unknown function and the dot over x stands for the differentiation with respect to t. The control parameters are ε, a, g (forcing amplitude) and and ω (forcing frequency).

Some aspects concerning canard bifurcations are analyzed in [Diener, 1979, 1] and [Diener, 1979, 2] for the periodically forced generalization of Rayleigh equation (1). From mathematical perspective the nonautonomous system of nonlinear ODEs associated with this equation is one of a class of periodically forced nonlinear oscillators, as the van der Pol (VP) and Bonhoeffer van der Pol (BVP) systems are. The behavior of these systems was much numerically investigated in [Flaherty and Hoppensteadt, 1978], [Mettin et al., 1993] and [Barns and Grimshaw, 1997], due to their applications in electronics and physiology.

With (1), the two-dimensional nonlinear non-autonomous system of ODEs

$$\begin{cases} \dot{x}_1 = x_2, \\ \dot{x}_2 = -\frac{a}{\varepsilon} x_1 + \frac{1}{\varepsilon} \left(x_2 - \frac{x_2^3}{3} \right) + \frac{g}{\varepsilon} \sin \omega t, \end{cases} \tag{2}$$

and the three-dimensional nonlinear autonomous system

$$
\begin{cases}
\dot{x}_1 = x_2, \\
\dot{x}_2 = -\frac{a}{\varepsilon}x_1 + \frac{1}{\varepsilon}\left(x_2 - \frac{x_2^3}{3}\right) + \frac{g}{\varepsilon}\sin x_3, \\
\dot{x}_3 = \omega \, mod \, 2\pi,
\end{cases}
\tag{3}
$$

are associated. A three-dimensional dynamical system with phase space $\mathbb{R}^2 \times S^1$ can be associated with (3). In [Sterpu et al., 2000], for the unforced case $g = 0$, the existence of a unique limit cycle for the dynamical system associated with the system,

$$
\begin{cases}
\dot{x}_1 = x_2, \\
\dot{x}_2 = -\frac{a}{\varepsilon}x_1 + \frac{1}{\varepsilon}\left(x_2 - \frac{x_2^3}{3}\right),
\end{cases}
\tag{4}
$$

for the case $a \cdot \varepsilon > 0$, is proved.

Therefore, the system (3) without periodic forcing ($g = 0$) exhibits a natural oscillation and we consider a sinusoidal forcing imposed on it ($g \neq 0$). Fixing the parameters ε, a, and g, as ω increases away from zero, the interaction between the frequencies of these two oscillations determines the resulting dynamics. Periodic as well as chaotic motion may occur.
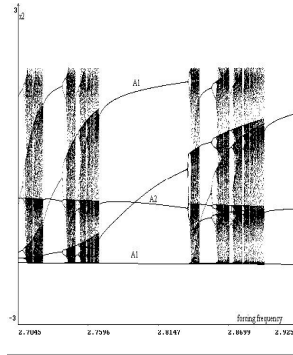
FIGURE 1. Bifurcation diagram for parameters ε=0.1250, a=0.5, g=0.6666 and $2.7045 \leq \omega \leq 2.9250$.

The lack of equilibria and the great number of parameters make the study of such a system difficult. Numerical methods often provide a useful and sometimes the only tool for study.

In this paper the aim of the numerical analysis is to establish ω intervals for which specific behaviour concerning the attractors of the system (3) could be expected. By logistic reasons we investigated a region in the four-dimensional parameter space (ε, a, g, ω) given by $0 < \varepsilon \leq 1$, $0 < a \leq 1$, $0 < g \leq 1$ and $2.7045 \leq \omega \leq 2.9250$. "Canard" bifurcations in the system (3) were studied in [Diener, 1979, 1] for the case $\omega = 1$ and $g = 0.6666$. This is the reason why we choose this value for the g parameter.

The diagnostics used to establish structural changes of the system (3) involve representations of solutions in the phase space $\mathbb{R}^2 \times S^1$, time series, Poincaré sections at intervals of forcing period $\frac{2\pi}{\omega}$, bifurcation diagrams with $\omega - x_2$ coordinates, evaluations of the eigenvalues of the linearized Poincaré map-matrix, evaluations of the Lyapunov exponents. All the numerical computations were carried out through the application of a variable step-size four order Runge-Kutta method [Băzăvan, 1999]. The 3D-representation uses a centre projection [Băzăvan, 1994].

The bifurcation diagram plotted in Fig. 1, for the case $\varepsilon = 0.1250$, $a = 0.5$, $g = 0.6666$ and ω in the interval $2.7045 \leq \omega \leq 2.9250$ shows the typical system behaviour which will be interpreted in the next sections.

The asymptotic results for $g \ll 1$ in (2), presented in Sec. 2, justify some results outlined in Secs. 4 and 5. The mathematical model used in our numerical study is presented in Sec. 3. The Sec. 4 is concerned with the numerical study of alternating periodic and chaotic attractors in the behaviour of the system (3). Aspects concerning metamorphoses of basin boundaries of co-existing periodic attractors are presented in Sec. 5.

2. Asymptotic results for $g \ll 1$

Here we put the nonautonomous system (2) in a form to which we can apply the averaging Theorem 4.1.1, [Guckenheimer and Holmes, 1983]. Then, from the dynamics of the averaged system we deduce results concerning the local dynamics of (2).
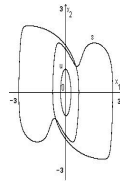
FIGURE 2. Stable (s) and unstable (u) limit cycles for (2) for parameter values $\varepsilon{=}0.1250$, $a{=}0.5$, $g{=}0.6666$ and $\omega{=}2.7802$.

First, we prove the following proposition.

Proposition 2.1. *[Băzăvan, 2001] The averaged system associated with the periodically forced system (2) for $g \ll 1$ is the unforced system (4).*

Proof Performing the time change $\tau = t/g$ and introducing the notation $\widehat{x}_1(\tau, g) = x_1(g\tau, g)$, $\widehat{x}_2(\tau, g) = x_2(g\tau, g)$ the system (2) reads

$$\begin{cases} \frac{d\widehat{x}_1}{d\tau} = g\widehat{x}_1, \\ \frac{d\widehat{x}_2}{d\tau} = g\left(-\frac{a}{\varepsilon}\widehat{x}_1 + \frac{1}{\varepsilon}\widehat{x}_2 - \frac{1}{3\varepsilon}\widehat{x}_2^2\right) + g^2 \sin \omega\tau g. \end{cases} \quad (5)$$

According to Guckenheimer [1983], the autonomous averaged system associated with (5) is

$$\begin{cases} \frac{d\widetilde{x}_1}{d\tau} = g\widetilde{x}_1, \\ \frac{d\widetilde{x}_2}{d\tau} = g\left(-\frac{a}{\varepsilon}\widetilde{x}_1 + \frac{1}{\varepsilon}\widetilde{x}_2 - \frac{1}{3\varepsilon}\widetilde{x}_2^2\right). \end{cases} \quad (6)$$

Next, performing in (6) the inverse time change $t = \tau \cdot g$, we obtain the system (4).

In [Sterpu et al., 2000] we proved that, for $a > 0$, $\varepsilon > 0$ the unforced system (4) possesses a unique hyperbolic equilibrium point $x = 0$, which is a repulsor, and a

unique hyperbolic attractive limit cycle Γ_0 surrounding the equilibrium. Based on Proposition 2.1 and Theorem 4.1.1 [Guckenheimer and Holmes, 1983], we obtain the following results.

Proposition 2.2. [4] *(i) There exists $g_0 > 0$ such that for all $0 < g \leq g_0$, the system (2) possesses a unique unstable hyperbolic periodic orbit $\Gamma_g(\tau) = \mathbf{0} + 0(g)$. (ii) There exists $g_1 > 0$ such that for all $0 < g \leq g_1$, the system (3) has a hyperbolic invariant torus T_g near $\Gamma_0 \times S^1$.*

Numerical computations showed that, for the parameter values chosen by us, such an unstable orbit exists indeed. In Fig. 2 the unstable periodic orbit is plotted together with the two co-existing stable orbits for the parameter values $\varepsilon = 0.1250$, $a = 0.5$, $g = 0.6666$, $\omega = 2.7802$. For $g = 0.6666$ and various ω values, the existence of invariant torus is numerically proved by the 3D-representations from Secs. 4 and 5.

3. The mathematical model

In order to present the mathematical model used in the numerical study from Secs. 4 and 5, we shortly write (3) in the form

$$\dot{x} = f(x), \tag{7}$$

where f is defined on the $\mathbb{R}^2 \times S^1$ cylinder.

We define the Poincaré map as follows. Let

$$\sum = \left\{ (x_1, x_2, x_3) \in \mathbb{R}^2 \times S^1, x_3 = 0 \, mod \frac{2\pi}{\omega} \right\}$$

be a surface of section [Băzăvan, 2001], which is transversally crossed by the orbits of (7). The Poincaré map $P : \sum \rightarrow \sum$ is defined by

$$P(\mathbf{x}_0) = \mathbf{x}(t, \mathbf{x}_0) = \int_0^{\frac{2\pi}{\omega}} f(\mathbf{x}(t, \mathbf{x}_0)) \, dt, \tag{8}$$

where $x_0 \in \sum$ and $x(t, x_0)$ is the solution of the Cauchy problem $x(0) = x_0$ for (7). We denote by P^n the n-times iterated map.

Let $\xi(t, x_0)$ be a periodic solution of (7) with period $T = n \cdot \frac{2\pi}{\omega}$, lying on a closed orbit and consider the map P of the initial point x_0. Then, to this closed orbit an n-periodic orbit of P corresponds. Numerically, the period T (i.e. n from the expression of T) can be determined by integrating Eq. (7) with the initial condition x_0 and sampling the orbit points $x_k = P(x_{k-1})$, $k \geq 1$ at discrete times $t_k = k \cdot \frac{2\pi}{\omega}$, until $P^k(x_0) = x_0$. Then, $n = k$ [Băzăvan, 2001].

The stability discussion of the periodic orbit $\xi(t, x_0)$ is reduced to the stability discussion of the fixed point x_0 of P^n, i.e. $P^n(x_0) = x_0$. The linear stability of the n-periodic orbit of P is determined from the linearized-map matrix DP^n of P^n. Using the Floqet theory [Reithmeier, 1991], [Glendinning, 1995] the matrix DP^n of P^n can be obtained by integrating the linearized system (7) for a small perturbation $y \in \mathbb{R}^2 \times S^1$. The time history of the initial perturbation $y(0) = y_0$ is described by the linearized ODE around the periodic solution ξ.

The stability of the periodic solution $\xi(t, x_0)$ is determined by the eigenvalues of the matrix DP^n [Reithmeier, 1991], [Glendinning, 1995], [Kuznetsov, 1998]. We note that one of the eigenvalues of this matrix always equals 1 [Glendinning, 1995], and that the remained two eigenvalues, also called the Poincaré map multipliers, influence the stability. We denote these eigenvalues by λ_1 and λ_2.

4. Bifurcations. Periodic and chaotic attractors
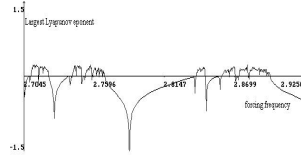
FIGURE 3. The largest Lyapunov exponent for (3), for parameter values ε=0.1250, a=0.5, g=0.6666 and $2.7045 \leq \omega \leq 2.9250$.
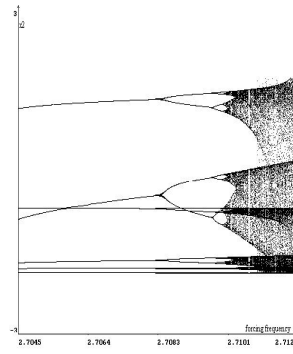
FIGURE 4. Bifurcation diagram for parameter values ε=0.1250, a=0.5, g=0.6666 and $2.7045 \leq \omega \leq 2.7120$.

In this section, by varying the parameter ω and keeping constant ε, a and g we study bifurcations associated with changes of stability in the periodically forced Rayleigh system (3).

The multipliers of the Poincaré map P^n, computed for $\varepsilon = 0.1250$, $a = 0.5$, $g = 0.6666$ and various ω values in the interval $2.7045 \leq \omega \leq 2.9250$, give information about the stability changes of an n-periodic orbit of (3) for which the map P is associated (see Sec. 3). Thus, the periodic orbit is stable only if $|\lambda_{1,2}| < 1$, [Reithmeier, 1991], [Glendinning, 1995], [Kuznetsov, 1998]. If, for a critical ω value, the multipliers satisfy $\lambda_1 = -1$, $-1 < \lambda_2 < 0$, [Reithmeier, 1991], [Glendinning, 1995], [Kuznetsov, 1998], the periodic orbit loses its stability through a period-doubling bifurcation. The motion becomes chaotic if, monotonically increasing ω, for sufficiently values, this process is repeated. This period doubling sequence leading to a chaotic state was reported in [Mettin, et al., 1993], [Barnes and Grimshaw, 1997] and [Sang-Yoon and Bumbi, 1998] for VP and BVP oscillators and inverted pendulum

respectively. We also note that the reverse process can occur for the case of an unstable orbit. That is, when a multiplier λ of an unstable orbit increases through -1 the orbit becomes stable via period-doubling bifurcations.

As Fig. 1 shows, the system (3) exhibits the mentioned period-doubling sequences. Obvious chaotic regions interrupt periodic windows and then, chaotic attractors replace periodic attractors due to a destabilisation process through a period-doubling sequence. The reverse process, the stabilisation one, determines that periodic attractors replace chaotic attractors [Băzăvan, 2001].
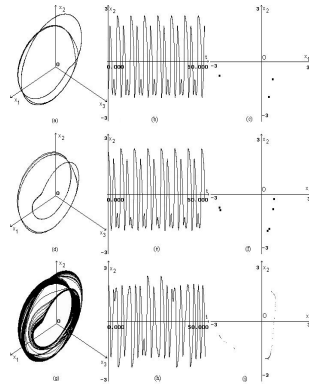
FIGURE 5. Closed trajectories, time series and Poincaré sections for system (3).

In order to ascertain these alternating regular and chaotic regions, the largest Lyapunov exponent measuring the convergence or divergence of neighbouring trajectories [Ott, 1993], [Barnes and Grimshaw, 1997] was plotted in Fig. 3 for the same parameter values as in Fig. 1. Negative values of this exponent correspond to periodic windows and positive values to chaotic regions.
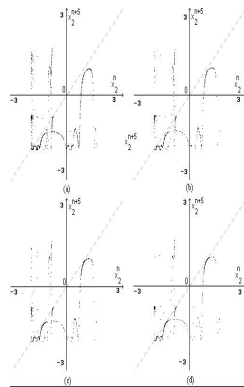
FIGURE 6. The points $\mathbf{X}_{n+5} = P^5(\mathbf{X}_n)$ for parameter values (a) $\omega=2.7225$, (b) $\omega=2.7230$, (c) $\omega=2.7235$, (d) $\omega=2.7240$.

In Fig. 4, which is a magnification of the bifurcation diagram in Fig. 1, for $2.7045 \leq \omega \leq 2.7120$, the typical route to chaotic state through a period-doubling sequence is more clearly seen. For $2.7045 \leq \omega < 2.7083$ two period-3 attractors

are present. The simultaneous presence of two attractors and the "jump" of the trajectories from one attractor to the other are characteristic to this system and is analysed in Sec. 5. Phase space with one of these period-3 solutions is represented on an invariant torus in Fig. 5a for $\omega = 2.7045$. For the solution in Fig. 5a, corresponding time series and Poincaré section with the three intersecting points are plotted in Figs. 5b-c. At $\omega \approx 2.7083$ the function curves split and the two solutions double their period as shows Fig. 4. The doubled periodic orbit, corresponding to those from Fig. 5a, is represented in Fig. 5d for $\omega = 2.7090$. From the time series and the Poincaré section, plotted in Figs. 5e-f, the period six of the limit cycle is obvious.

The first period-doubling bifurcation at $\omega \approx 2.7083$ is followed by many subsequent period-doubling bifurcations. The length of the intervals of ω between these bifurcations decreases. Using magnifications of bifurcation diagram in Fig. 4, smaller ω step (i.e. 10^{-6}) and computing the $\lambda_{1,2}$ multipliers, for this period-doubling cascade the first five terms of the Feigenbaum progression $\frac{\omega_i - \omega_{i-1}}{\omega_{i+1} - \omega_i}$, [Kuznetsov, 1998], were estimated : 5.25, 5.18, 4.95, 4.81 and 4.72 [Băzăvan, 2001]. The convergence to the universal constant 4.6692 of this decreasing sequence is followed.

For $2.7106 < \omega < 2.7240$ the behaviour of the system is chaotic. The chaotic attractor, corresponding time series and Poincaré section are represented in Figs. 5g-i for $\omega = 2.7120$. At this ω value the largest Lyapunov exponent was computed to be 0.1812 [Băzăvan, 2001] providing the chaotic state of the system. As Fig. 1 shows, for $\omega \approx 2.7240$, the chaotic attractor is replaced by a period-5 attractor. In order to illustrate this change from a chaotic attractor to a periodic attractor, the sequences of x_2 coordinates of the points $\mathbf{X}_{n+5} = P^5(\mathbf{X}_n)$ are plotted in Figs. 6a-d [Băzăvan, 2001].

For $\omega = 2.7225$ the diagonal $x_2^{n+5} = x_2^n$ is intersected in three separate locations. Here x_2^n represents the x_2 coordinate of the point $\mathbf{X}_n$. A channel between the diagonal and the return map curve is observed. As ω increases, the return map curve approaches the diagonal and at $\omega = 2.7240$ it is tangent in five distinct locations. A saddle-node bifurcation is encountered. The chaotic attractor is abruptly destroyed and replaced by a period-5 attractor. Note that, as the ω parameter increases, the density of the return points grows in the regions of the future attractor and diminishes in the other ones. This measure of the return points changes continuously with the continuous variation in the control parameter.

5. Metamorphoses of basin boundaries

It is known that, dynamical systems associated with nonlinear ODEs may possess more than one periodic or/and chaotic attractors who exist simultaneously [Barnes and Grimshaw, 1997]. Thus, for particular parameter combinations the response of the dynamical system is sensitively dependent on the initial conditions and the resulting motion could be on any of these attractors. In addition, separatrices between the attraction basins may be nonsmooth curves (i.e. fractal basin boundaries). In such cases, predictability becomes impossible because small variations in the initial conditions may determine different dynamics on distinct attractors [Barnes and Grimshaw, 1997].

Basin boundaries metamorphoses, reported in [Grebogi et al., 1986], [Barnes and Grimshaw, 1997], can be also observed in the case of dynamical system associated with (3) [Băzăvan, 2001]. In the bifurcation diagram in Fig. 8, two period-2 attractors, denoted by A1 and A2, are present for $2.7680 < \omega < 2.8382$. Both limit cycles
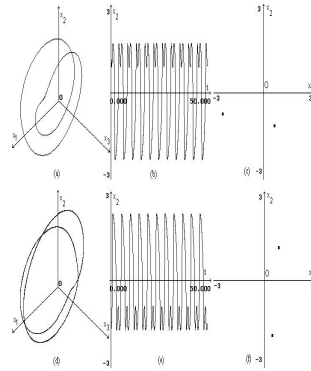
FIGURE 7. Closed trajectories, time series and Poincaré sections for parameters ε=0.1250, a=0.5, g=0.6666 and ω=2.7802 and initial points (a)-(c) (1,0,0) and (0.4577,0,0) ; (d)-(f) (1,1,0) and (0.5231,0,0).
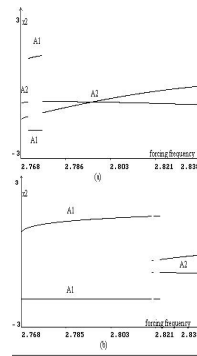
FIGURE 8. Bifurcation diagram for (3) for parameters ε=0.1250, a=0.5, g=0.6666 and ω=2.7802 and initial points (a)(1,0,0) ; (b) (1,1,0).

situated on invariant tori, corresponding time series and Poincaré section points are plotted in Figs. 7a-c and 7d-f for $\omega = 2.7802$.

More precisely, we started with $\omega = 2.7680$. For a small (of order 10^{-4}) increase in ω, the trajectory "jumps" from A2 to A1 and conversely, from A1 to A2. This phenomenon is observed in Figs. 8a-b where Poincaré section points of trajectory starting from $(1,0,0)$ and $(1,1,0)$, respectively, are represented in the $\omega - x_2$ plane. For the interval $2.6820 \leq \omega < 2.7712$ the trajectory starting from $(1,0,0)$ is on the attractor A2 and at $\omega \approx 2.7712$ it "jumps" on A1.

The reverse jump is observed at $\omega \approx 2.7764$. Note that, the values of ω for these "jumps" are very much sensitive on the initial conditions. See Figs. 8a-b for the difference. Also, as observed in Figs. 7a-b and 7d-e, trajectories starting at the closed points $(0.4577, 0, 0)$ and $(0.5231, 0, 0)$ are on the attractor A1 and A2 respectively.

The "jumping" phenomenon follows from a discontinuous structural change of basin boundaries associated with the attractors A1 and A2.
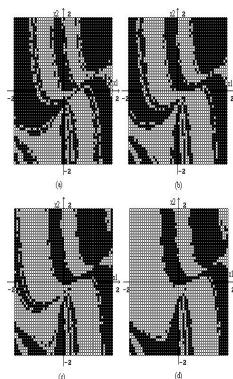
FIGURE 9. Basins of attraction for two limit cycles of (3), for parameters values (a) $\omega=2.7710$, (b) $\omega=2.7720$, (c) $\omega=2.7770$, (d) $\omega=2.7800$.

In Figs. 9a-d a sequence of diagrams of the basins of attraction associated with A1 and A2 are plotted for $\omega = 2.7710$, $\omega = 2.7720$, $\omega = 2.7770$ and $\omega = 2.7800$. In each case the black circles represent the basin of attraction for A1 and the white circles the basin of attraction for A2. Significant changes of the basin boundaries are observed when ω increases. The behavior of the system is periodic although the basin boundaries seem to be fractal in nature. This fact is also outlined in [Grebogi et al., 1986] in the case of a forced damped pendulum.

Conclusions

The numerical study in this paper shows that the periodically forced Rayleigh system possesses a lot of phenomena encountered in many other nonlinear systems. Some of them as period-doubling and saddle-node bifurcations, alternating periodic and chaotic attractors, simultaneous presence of more than one periodic attractors and metamorphoses of their basin boundaries were outlined here. In particular, the existence of standard attractors with fractal boundaries is emphasized.

References

[1] B. Barnes and R. Grimshaw [1997], *Numerical studies of the periodically forced Bonhoeffer van der Pol oscillator*, Int. J. Bifurcation and Chaos, 7(12), pp. 2653–2689.

[2] P. Băzăvan [1994], *Problems of Computational Geometry in "Ray-tracing"*, Annals of University of Craiova, Romania, Math. Comp. Sci. Series XX, pp. 80–88.

[3] P. Băzăvan [1999], *The dynamical system generated by a variable step size algorithm for Runge-Kutta methods*, Int. J. Chaos and Theory and Applications, 4(4), pp. 21–28.

[4] P. Băzăvan [2001], *Tridimensional Computation Study of Attractors for van der Pol - type Equations*, Ph.D. thesis, Institute of Mathematics of Roumanian Academy, Bucharest, Romania.

[5] M. Diener [1979], *Nessie et les canards*, IRMA, Strasbourg.

[6] M. Diener [1979], *Quelques examples de bifurcations et les canards*, Publ. IRMA, pp. 37.

[7] J.,E. Flaherty and F.,C. Hoppensteadt [1978], *Frequency entrainment of a forced van der Pol oscillator*, Studies Appl. Math, 58, pp. 5–15.

[8] P. Glendinning [1995], *Stability, Instability and Chaos*, Cambridge, New York.

[9] E. Grebogi, E. Ott and J. Yorke [1986], *Metamorphoses of basin boundaries in nonlinear dynamical systems*, Phys. Rev. Lett., 56(10), pp. 1011–1014.

[10] J. Guckenheimer and P. Holmes [1983], *Nonlinear oscillations, dynamical systems and bifurcations of vector fields*, Springer, New York, pp. 168.

[11] Y. Kuznetsov [1998], *Elements of applied bifurcation theory*, Springer Verlag, New York.

[12] R. Mettin, U. Parlitz and W. Lauterborn [1993], *Bifurcation structure of the driven van der Pol oscillator*, Int. J. Bifurcation and Chaos, 3(6), pp. 1529–1555.

[13] E. Ott [1993], *Chaos in dynamical systems*, Cambridge University Press.

[14] E. Reithmeier [1991], *Periodic Solutions of Nonlinear Dynamical Systems*, Springer Verlag.

[15] Kim Sang-Yoon and Uh. Bumbi [1998], *Bifurcations and Transitions to Chaos in an Inverted Pendulum*, Electronic paper.

[16] M. Sterpu and P. Băzăvan [1999], *Study on a Rayleigh equation*, Annals of University of Pitesti, Romania, Math. Comp. Sci. Series, 3, pp. 429–434.

[17] M. Sterpu, A. Georgescu and P. Băzăvan [2000], *Dynamics generated by the generalized Rayleigh equation II. Periodic solutions*, Mathematical Reports, 2(52), pp. 367–378.

(Petre Băzăvan) Department of Informatics, University of Craiova,
Al.I. Cuza Street, No. 13, Craiova RO-200585, Romania, Tel. & Fax: 40-251412673
E-mail address: bazavan@yahoo.com